Available online at www.sciencedirect.com

ScienceDirect

Procedia Manufacturing 50 (2020) 749–756

Procedia MANUFACTURING

www.elsevier.com/locate/procedia

18th International Conference Metal Forming 2020

Characterization, modeling and microstructure of composite aluminium alloy specimens after ECAP

Carlo Bruni[a,]*, Daniele Ciccarelli[a]

[a]*DIISM, Università Politecnica delle Marche, Via Brecce Bianche, Ancona 60131, Italy*

* Corresponding author. Tel.: +39-071-220-4291; fax: +39-071-220-0000. *E-mail address:* c.bruni@univpm.it

Abstract

The ECAP, the Equal Channel Angular processing or pressing, in general allows to modify the properties of materials at the microstructure level. In the proposed investigation, the composite specimens in aluminium alloy were subjected to different ECAP passes. The characterization after ECAP was performed by means of warm compression tests between 200 and 300°C with different ram velocities.
By a coupled experiment-analytical methodology the friction effect was quantified and the stress-strain curves reported for different temperatures, deformation velocities and ECAP conditions. The friction effect was isolated and the flow behaviour trend of the alloy under different conditions modeled with two models. In particular a model in which the friction variable was considered and the other one in which the friction variable was completely neglected were built and tested. The countertrends in the initial ECAP passes were analyzed by microstructure investigation. The behaviour of the alloy under the considered conditions can be effectively modeled once identified the correct parameters in terms of pre-deformation.

Keywords: ECAP, compression test, friction, temperature, modeling, Aluminium alloy.

1. Introduction

The Equal Channel Angular Processing or pressing represents an heavy deformation of the material typical of many cold forming processes, for example at the flash level during forging or extrusion.

Nomenclature

ECAP Equal Channel Angular Processing
CDRX Continuous Dynamic Recrystallization
DRX Dynamic Recrystallization
GDRX Geometric Dynamic Recrystallization

Such pre-deformation can be performed in order to produce a change in the material from the microstructure point of view [1-6] useful to get a component respecting given requirements or to realize a subsequent warm stamping.

The effect of ECAP passes on the wear resistance of the alloy is reported in [6,7] in which the decrease in the wear resistance of the material with increasing the number ECAP passes is detailed.

In [8] the simultaneous improvement in stress and ductility that can be reached when starting from grain dimension of about 200-300 microns is described. In [9,10], the effect of the number of ECAP passes on the flow behaviour of the alloy in terms of stress and workability is reported. Such behaviour was studied at temperatures higher than the room one.

In other words, considering that the extruded rods or in general pre-deformed workpieces are subjected to further deformation, the cold pre-deformation could be used to produce

2351-9789
10.1016/j.promfg.2020.08.135

the accumulated strain useful to get the desired strength and workability [11].

In detail, the accumulated previous deformation can in general produce a microstructure change in terms of grain dimensions due to subgrain mis-orientation, development and accumulated dislocations. The related internal stress in the material could be solvable with a subsequent in temperature deformation. The phenomenon due to the temperature rising [12], consisting in dislocation motion at the grain and subgrain boundaries, could determine a subgrain growth into adjacent grains. The result of that produces under some conditions a change in grain size and restoration phenomena.

When the mis-orientation of subgrains and dislocation density is high under some conditions of deformation and/or temperature new grains are originated from the old strongly deformed grains. That means new undeformed grains [13,14]. In [15-19] the researchers reported the typical behaviour of 6000 series aluminium alloys during hot working in which continuous dynamic recrystallization (CDRX) prevails while fully Dynamical Recrystallization (DRX) takes place around 500°C with strain rates less than 0.1 1/s. However, for 6000 alloys is useful to consider the geometrical dynamic recrystallization in which the new grains are originated by the fragmentation of old grains while the DRX is considered as a nucleation. But, at low temperatures, the mis-orientation of subgrains is not always sufficient to justify new originated grains.

In general, the main different effects detectable when ECAP processing and subsequently warm forming aluminium alloys [20-22] can be reported as follows:

- The first effect due to the accumulated deformation typical of cold severe stages
- The non-uniform pre-deformation along the section of the billet from the centre to the periphery
- The effect of warm conditions due to temperature and strain rates
- The friction at the tool-workpiece contact interface that can affect the shape of the flow curves

Up today, the behaviour of the 6000 alloy under warm conditions and at strain rates less than 0.1 1/s appears far to be clear. In particular, the intensive pre-deformation given by cold ECAP on specimens subsequently subjected to warm deformation needs to be further investigated.

The present paper aims at investigating the effect of different ECAP passes on the microstructure and flow behaviour of the composite AA 6000 alloys tested with a warm compression test.

By a coupled experiment-analytical methodology the friction effect was quantified and the stress-strain curves reported for different ECAP conditions, temperature and deformation velocities. The friction effect was isolated and the flow behaviour trend of the alloy under different conditions modeled with two equations: the one in which friction variable was considered and the other one in which the friction variable was completely neglected. Some countertrends in the initial ECAP passes were analysed by microstructure investigations.

The results, in terms of microstructure investigation, warm compression testing and modeling are reported in detail.

2. Methodology

The methodology adopted in the present investigation is reported in Fig. 1. It consists in a coupled experiment-analytical approach in which warm compression tests were performed on aluminium alloys previously pre-deformed by ECAP in order to model their behaviour.

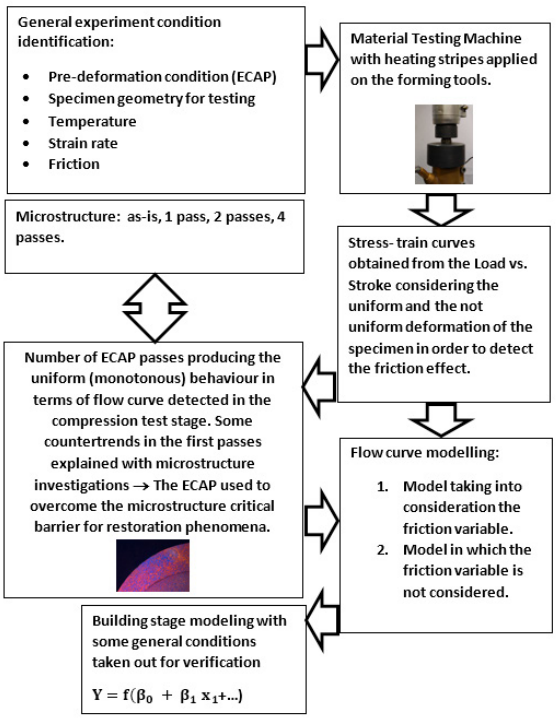

Fig. 1. Methodology.

2.1. Details of the experiment procedure

The cylindrical bimetallic rods in aluminium alloy AA6026-6012 were subjected to different ECAP passes with the geometry and in the conditions reported in [7,20] with the main angle of the matrix equal to 90°. The external diameter of the composite billet to be pre-deformed was 10.9 mm while the internal diameter of the tubular part was 7.8 mm. For each pass the microstructure information was detected. After pre-deformation the cylindrical elements were subject to warm compression tests in the temperature interval of 200-300°C using heating strips applied on the forming tools. This configuration was adopted in order to produce an increased uniform heating of the specimen, a contained heated volume and a faster heating with reduced energy required to reach and to maintain the objective temperature.

The testing equipment is shown in Fig. 2 in which the warm compression testing phase is reported. Three thermocouples were used: two on the heating strips and one the specimen prior to start the compression test.

Fig. 2. Testing equipment for warm compression tests.

The methodology reported the conditions of the initial specimen in terms of pre-deformation levels, related to the number of ECAP passes, and of the geometry of the composite aluminium alloy in order to get of stress-strain curves. The problem in compression test is represented by the friction that can produce a distorted information in terms of the flow behaviour of the material due to the generated geometry [21]. The use of theorical deformation of the specimen, id est without the barreling effect, allowed to separate the no friction condition from that of friction. In this way it is possible to obtain the real flow behaviour of the alloy. The temperature and the nominal deformation of about 30% selected allowed to get the deformation to the specimen after ECAP useful to contain as possible the effect of friction.

Of course the pre-deformation condition plays a key role in the identification of the flow behaviour of the material. The different pre-deformation levels imposed allowed to identify some countertrends in the first passes. The critical pass in which the microstructure change barrier can be overcome was better explained by microstructure investigation.

The specimens characterized by the initial ECAP conditions were subjected to microstructure investigation.

2.2. Details of the modeling

The analytical modeling was done on the flow behaviour of the alloy under different conditions of pre-deformation, friction, temperature and deformation velocity i.e. strain rate. Two equations were proposed. The first equation was used in practice to separate and to model the friction effect during compression test. The first equation was [20]:

$$Y = \exp(\beta_0 + \beta_1 x_1 + \beta_2 x_2 + \beta_3 x_3 + \beta_4 x_4 + \beta_5 x_5 + \beta_6 x_6 + \varepsilon') \quad (1)$$

where :

- $Y = \sigma$
- $\beta_0, \beta_1, \beta_2, \beta_3, \beta_4, \beta_5, \beta_6$ = coefficients of the equation
- $x_1, x_2, x_3, x_4, x_5, x_6$ = independent variables
- ε' = whole standard error

Considering that the friction variable could be completely neglected because strictly dependent on the testing conditions, a second equation was proposed:

$$Y = \exp(\beta_0 + \beta_1 x_1 + \beta_2 x_2 + \beta_3 x_3 + \beta_4 x_4 + \beta_5 x_5 + \varepsilon') \quad (2)$$

where :

- $Y = \sigma$
- $\beta_0, \beta_1, \beta_2, \beta_3, \beta_4, \beta_5$= coefficients of the equation
- x_1, x_2, x_3, x_4, x_5 = independent variables
- ε' = whole standard error

An iterative approach allowed to determine the form of the equations in terms of the number and variable typology. The variables of the equation (1) and of equation (2) are reported in Table 1 and in Table 2.

Table 1. Variables of the proposed equation (1).

Variables	Testing components	Conditions
x_1		-1/1(pre-deformation condition)
x_2	T, temperature in °C	
x_3		-1/1 (friction condition)
x_4	ε	
x_5	ε^5	
x_6	$Ln\left(\dot{\varepsilon} \cdot \exp\left(\frac{1}{8.31 \cdot T}\right)\right)$	

Table 2. Variables of the proposed equation (2).

Variables	Testing components	Conditions
x_1		-1/1(pre-deformation condition)
x_2	T, temperature in °C	
x_3	ε	
x_4	ε^5	
x_5	$Ln\left(\dot{\varepsilon} \cdot \exp\left(\frac{1}{8.31 \cdot T}\right)\right)$	

For both the equations a *t* test was used for verifying the significance of each variable. It was performed calculating the ratio between the coefficient and the standard error got to calculate it and comparing to each other the obtained values.

2.3. Details of prediction performance of modeling

The whole standard error was calculated by the root square of the mean square error.

The prediction performance of the two equations was also quantified by the following proposed index, plotted versus deformation:

$$\text{Prediction performance} = 1 - \left| \frac{\sigma_{equation} - \sigma_{\exp}}{\sigma_{\exp}} \right| \quad (3)$$

Where the $\sigma_{equation}$ is the equivalent stress calculated with equation (1) and with equation (2) while the σ_{exp} represents that given by the experiments.

3. Results

3.1. Microstructure investigations

The pre-deformation imposed to the material before warm forming influences the subsequent deformation. The attitude of ECAP in modifying the microstructure depends on the ECAP configuration. In Fig. 3, it is possible to observe the general structure of the specimen after pre-deformation 1 and after pre-deformation 4. The internal part of the composite material appears less deformed as also found by other authors [6, 23]. The specimen appears strongly deformed with a deformation evident in the zone of external part reported in Fig. 3 (b).

In Fig. 4, different conditions in terms of pre-deformation are reported starting form the as-is material shown in Fig.4 (a).

In particular, after the first pre-deformation the normal strain-hardening configuration due to the accumulated cold deformation is detected even though at not high deformation levels. In Fig. 4 (b) it is possible to observe a distortion and re-orientation of the grains that is not sufficient to produce a real grain size refinement. Furthermore, also the precipitation dispersion is detectable from Fig. 4 (a) to Fig. 4 (b). After the pre-deformation 2 the accumulated strain increases and the grain deformation and the subgrain mis-orientation already produced takes place until a peak of dislocation density and then of internal stress. That is the condition of the critical mis-orientation. After pre-deformation 4 the cold subgrain mis-orientation increases determining the conditions of fragmentation and sometimes microvoids generation originating something similar to new grains. That is a not stable configuration.

The subsequent increase in temperature during compression testing allows to adjust the dislocation density configuration and to start the static and dynamic restoration phenomena able to get the flow behaviour of the material reported in Fig. 5. The results are similar to those of warm ECAP found by other authors [22-24].

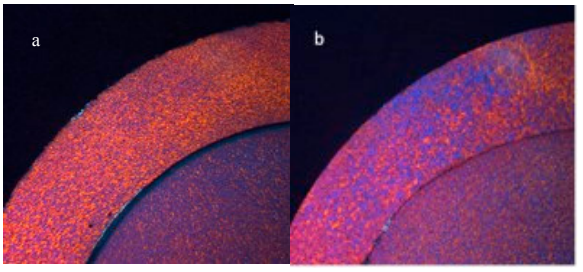

Fig. 3. The whole specimen deformed: (a) after pre-deformation 1; (b) after pre-deformation 4.

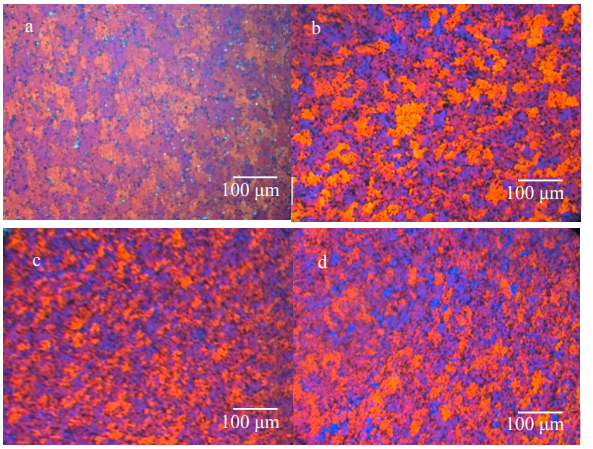

Fig. 4. Microstructure of pre-deformed specimens: (a) as-is; (b) after pre-deformation 1; (c) after pre-deformation 2; (d) after pre-deformation 4.

In detail, at the highest temperature and strain rate i.e. 300°C and 0.01 1/s investigated, the effect of pre-deformation 2 is represented by a slight increase in the flow stress at the beginning of deformation with respect to the condition of pre-deformation 1. Such slight increase was not confirmed in the subsequent pre-deformation passes. The pre-deformation 2 represents, under the condition of the present investigation, the critical barrier that can be overcome imposing subsequent pre-deformations to the billet. Such countertrends were also detected by other authors [10, 25].

In detail, in that pass the static and dynamic restoration phenomena begin, due to both the pre-deformation condition and to the temperature level being the latter very near to hot forming threshold [15-18].

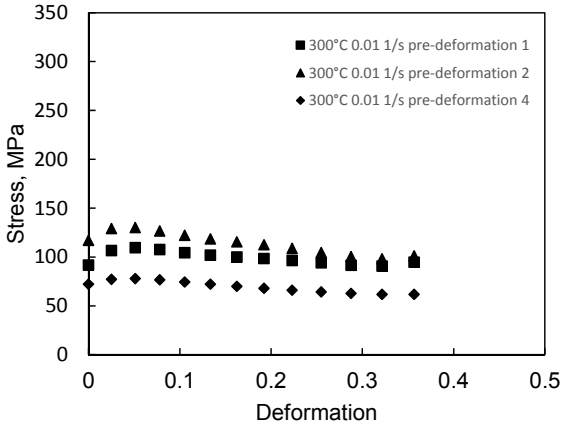

Fig. 5. Flow curve behaviour of specimens after pre-deformation 1, 2 and 4 compressed at 300°C and 0.01 1/s.

In order to better understand the material behaviour also under warm forming conditions the friction effect needs to be evidenced and separated. The obtained flow curves under warm and friction conditions are reported in the following Figures 6 and 7.

Instead, in the Figures 8 and 9 the comparison between the flow curves got after the first and after the fourth pre-deformation pass are reported, without the effect of friction.

3.2. Modeling and performance evaluation

The modeling phase got the objective to perform the description of the flow behaviour of the alloy taking into account the friction variable to be tuned in the equation (1) and without the friction variable in the equation (2). The coefficient and their significance are reported in Table 3 and Table 4.
In Figures 10 and 11 the comparison between the two equation (1) and (2) in predicting the flow curve shape and levels is reported. A very good agreement between prediction and experiment results can be observed. The standard errors related to the equation (1) and (2) were represented by the square root of the mean square error. For the equation (1) it was equal to 0.052. Being equal to 1.052 MPa. For the equation (2) the standard error was equal to 0.043, that means equal to 1.043 MPa. Due to the extremely low values they were not considered in the generation of the predicted flow curves.

Table 3. Coefficients of the proposed equation (1).

Coefficients	Values	Significant
β_0	8.5703	133.7019
β_1	-0.1722	-34.3838
β_2	-0.0114	-86.0548
β_3	0.0267	5.9660
β_4	-0.1862	-2.7105
β_5	-13.7048	-3.0352
β_6	0.1421	24.6972

Table 4. Coefficients of the proposed equation (2).

Coefficients	Values	Significant
β_0	8.4396	110.7878
β_1	-0.1725	-28.9745
β_2	-0.0111	-70.8562
β_3	-0.3364	-4.1205
β_4	-12.9676	-2.4165
β_5	0.1314	19.1952

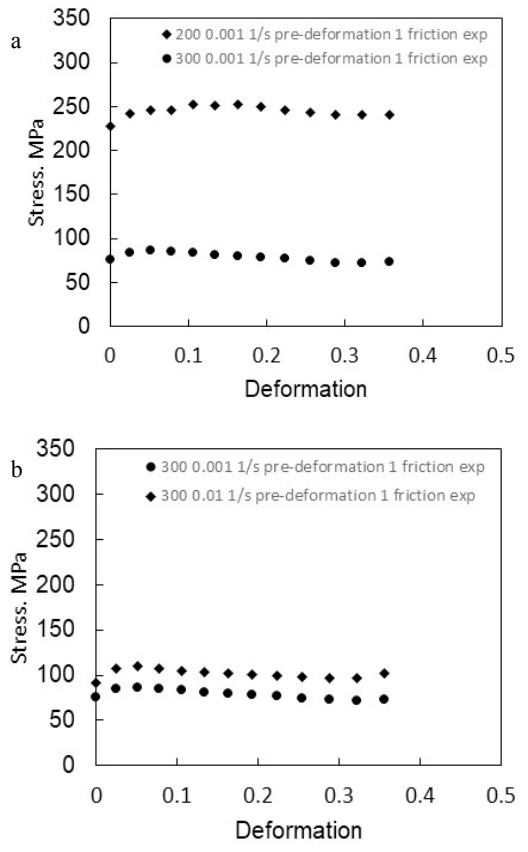

Fig. 6. Flow curve behaviour after pre-deformation 1 with the friction: (a) main effect of temperature; (b) main effect of strain rate.

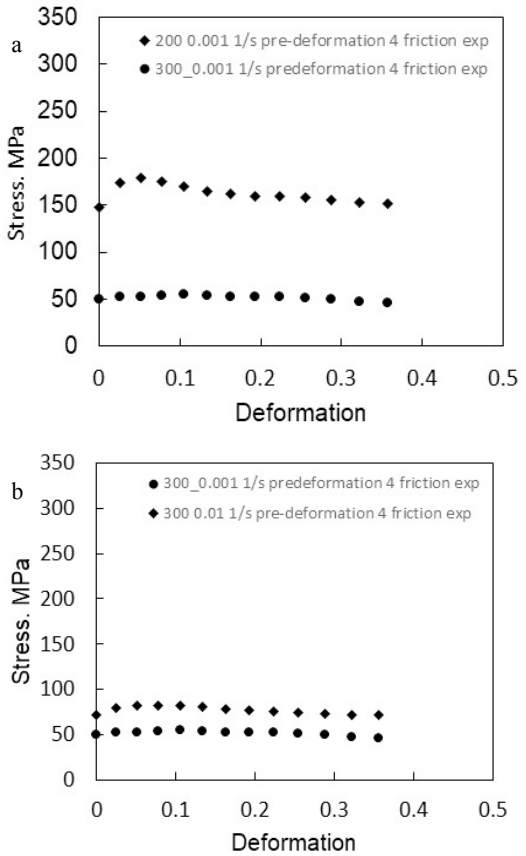

Fig. 7. Flow curve behaviour after pre-deformation 4 with the friction: (a) main effect of the temperature; (b) main effect of strain rate.

In order to get a whole comparison between equation (1) and equation (2) the modeling evaluation was reported in terms of prediction performance shown in Fig. 12.

In Fig. 13 the comparison between curves predicted by the two equations and a curve not used in the building phase, obtained at 300°C 0.001 1/s, can be seen.

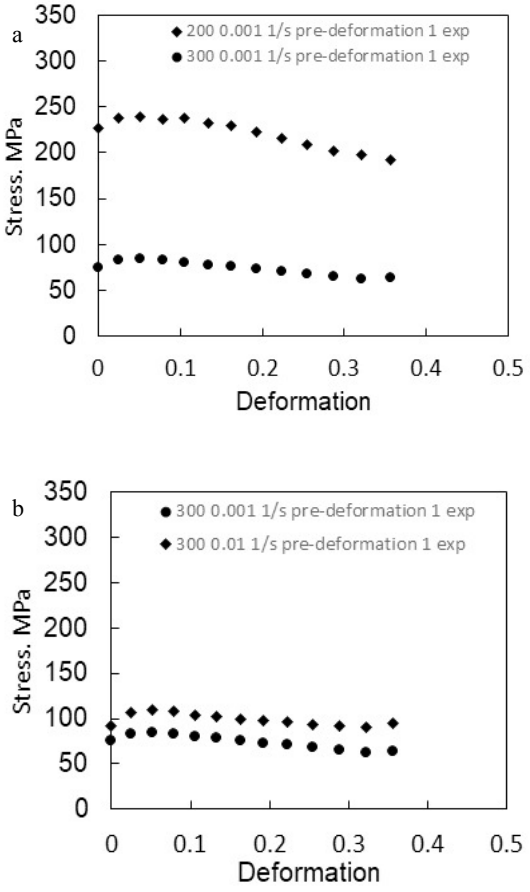

Fig. 8. Flow curve behaviour after pre-deformation 1 obtained without friction: (a) main effect of temperature; (b) main effect of strain rate.

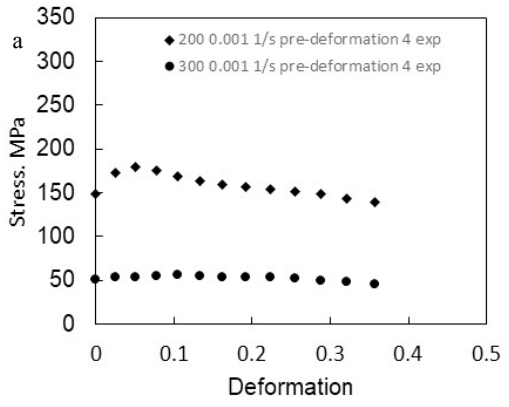

Fig. 9. (See below)

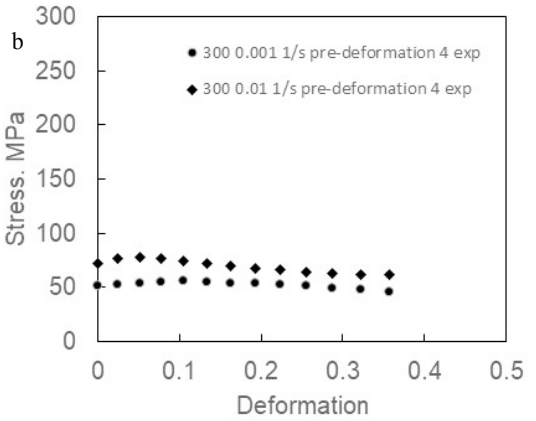

Fig. 9. Flow curve behaviour after pre-deformation 4 obtained without friction: (a) main effect of the temperature; (b) main effect of the strain rate (b).

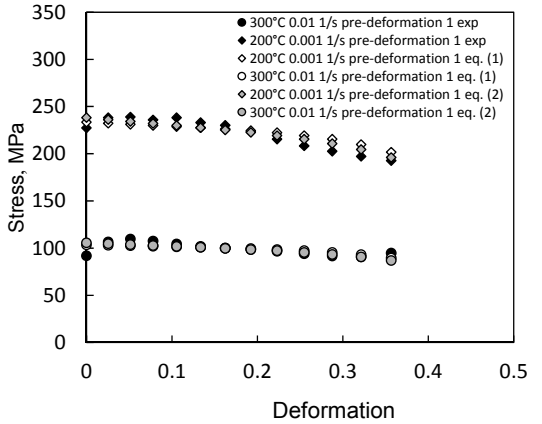

Fig. 10. Flow curve behaviour after pre-deformation 1 obtained without friction modeled with equation (1) and equation (2).

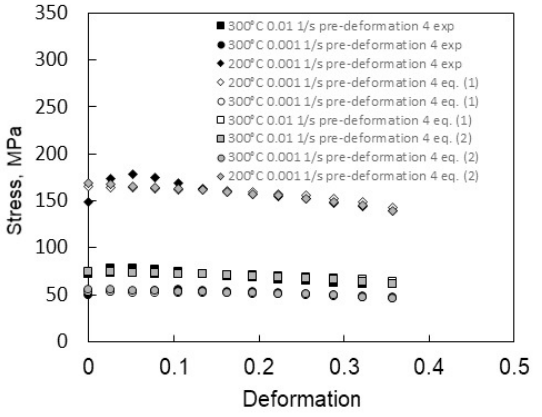

Fig. 11. Flow curve behaviour after pre-deformation 4 obtained without friction modeled with equation (1) and equation (2).

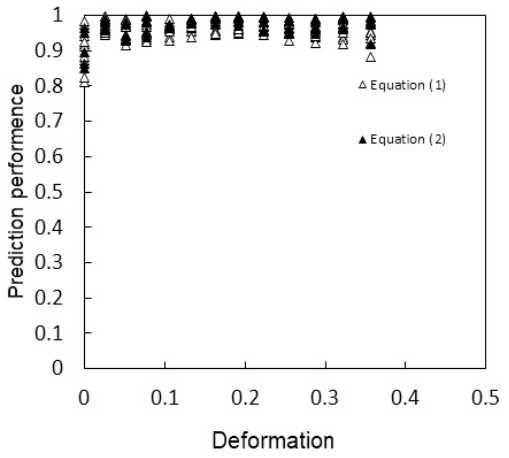

Fig. 12. Comparison between the prediction performance of the equation (1) and equation (2) in terms of the prediction performance.

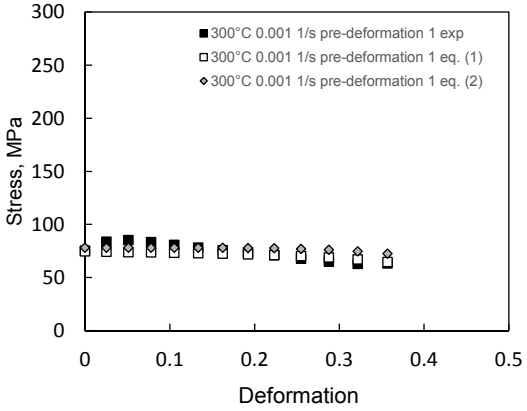

Fig. 13. Flow curve behaviour after pre-deformation 1 obtained without friction modeled with equation (1) and equation (2) in a testing condition not used in the building stage.

4. Conclusions

The present investigation aimed mainly at study the effect of the cold pre-deformation level on the flow behaviour of a composite alloy obtained under warm conditions.

It was observed, that:

- The accumulated strain produces along the subsequent ECAP passes mis-orientations of subgrains, increase in the dislocation density and dispersion of precipitate leading to old grain fragmentation;
- Some countertrends were detected in the first pre-deformation passes and attributed to the critical conditions achieved in terms of subgrain mis-orientation;
- The contribution of friction at tool-workpiece contact interface during warm compression was separated neglecting the barreling effect;
- The modeling of the flow curve behaviour obtained by warm compression test was performed by two equations differing from each other in the friction variable;
- Both the equations (1) and (2) were useful in predicting the flow behaviour of the alloy with errors of 1.052 MPa and 1.043 MPa, respectively;
- The simplification proposed in the equation (2) allows to better manage and describe the flow curve behaviour of the alloy under different conditions in terms of pre-deformation level, temperature and strain rates.

The proposed methodology based on microstructure investigation and on modeling of flow curves allowed to study in depth the material under different ECAP passes and its behaviour during warm forming under the conditions of the present investigation.

Acknowledgements

Authors wish to acknowledge the special work performed by Eng. M. Pieralisi. The UNIVERSITA' POLITECNICA DELLE MARCHE is also acknowledged for funding this research.

References

[1] Chrominski W, Olejnik L, Rosochowski A, Lewandowska M. Grain refinement in technically pure aluminium plates using incremental ECAP processing. Mater Sci Eng A 2015;636:172–80.
[2] Avcu E. The influences of ECAP on the dry sliding wear behaviour of AA7075 aluminium alloy. Tribology Int 2017;110:173–84.
[3] Duan Y, Tang L, Xu G, Deng Y, Yin Z. Microstructure and mechanical properties of 7005 aluminum alloy processed by room temperature ECAP and subsequent annealing. J Alloy Compd 2016;664:518–29.
[4] Veveçka A, Cabibbo M, Langdon T. A characterization of microstructure and microhardness on longitudinal planes of an Al–Mg–Si alloy processed by ECAP. Material Characterization 2013;84:126–33.
[5] Cabibbo M. Microstructure strengthening mechanisms in an Al–Mg–Si–Sc–Zr equal channel angular pressed aluminium alloy. Appl Surface Sci 2013;281:38–43.
[6] Estrin Y, Vinogradov A. Extreme grain refinement by severe plastic deformation: A wealth of challenging science. Acta Mater 2013;61:782-817.
[7] Bruni C, Cabibbo M, Ciccarelli D, Paoletti C. Characterization of double aluminium alloy specimens after ECAP. Procedia Manufacturing 2018;15:1517–24.
[8] Samaee M, Najafi S, Eivani A R, Jafarian H R, Zhou J. Simultaneous improvements of the strength and ductility of fine-grained AA6063 alloy with increasing number of ECAP passes. Mater Sci Eng A 2016;669:350–7.
[9] Mckenzie PWJ, Lapovok R. ECAP with back pressure for optimum strength and ductility in aluminium alloy 6016. Part 1: Microstructure. Acta Mater 2010;58:3198–211.
[10] Mckenzie PWJ, Lapvok R. ECAP with back pressure for optimum strength and ductility in aluminium alloy 6016. Part 2: Mechanical properties and texture. Acta Mater 2010;58:3212–22.
[11] Elhefnawey M, Shuai GL, Li Z, Nemat-Alla M, Zhang DT, Li L. On achieving superior strength for Al-Mg-Zn alloy adopting cold ECAP. Vacuum.
[12] Huang C-Q, Diao J-P, Deng H, Li B-J, Hu X-H. Microstructure evolution of 6016 aluminum alloy during compression at elevated temperatures by hot rolling emulation. Trans. Nonferrous Met. Soc. China 2013;231:576-1582.
[13] Aydi L, Khlif M, Bradai C, Spigarelli S, Cabibbo M, El Mehtedi M.

Mechanical properties and microstructure of primary and secondary AA6063 aluminum alloy after extrusion and T5 heat treatment. Materials Today: Proceedings 2015;2:4890–7.
[14] Vandermeer RA, Juul Jensen D, Recrystallization in hot vs colddeformed commercial aluminum: a microstructure path comparison. Acta Mater 2003;51:3005–18.
[15] Chamanfar A, Alamoudi M T, Nanninga N E, Misiolek W Z. Analysis of flow stress and microstructure during hot compression of 6099 aluminum alloy(AA6099). Mater Sci Eng A 2019;743:684-96.
[16] Spigarelli S, Evangelista E, McQueen H J. Study of hot workability of a heat treated AA6082 aluminum alloy. Scripta Mater 2003;49:179–83.
[17] Zhao J, Deng Y, Tang J, Zhang J. Influence of strain rate on hot deformation behavior and recrystallization behavior under isothermal compression of Al-Zn-Mg-Cu alloy. J Alloy Compd 2019;809:151788.
[18] Bruni C, Forcellese A, Gabrielli F. Flow Modelling of AA 6082 Aluminium Alloy. In: E. Kuljanic Ed. Proceedings of the 6th International Conference on Advanced Manufacturing Systems and Technology, Udine; 2002. p. 367-374.
[19] Shuhui L, Qinglin P, Mengjia L, Xiangdong W, Xin H, Xinyu L, Zhuowei P, Jianping L. Microstructure evolution and physical-based diffusion constitutive analysis of Al-Mg-Si alloy during hot deformation. Materials & Design 2019;184:108181.
[20] Bruni C, Ciccarelli D. Modeling of friction behaviour during in temperature compression tests on aluminium alloys. AIP Conference Proceedings 2019;2113:040017.
[21] Fan X G, Dong Y D, Yang H, Gao P F, Zhan M. Friction assessment in uniaxial compression test: A new evaluation method based on local bulge profile. J Mater Process Tech 2017;243:282–291.
[22] Mazurina I, Sakai T, Miura H, Sitdikov O, Kaibyshev R. Effect of deformation temperature on microstructure evolution in aluminium alloy 2219 during hot ECAP. Mater Sci Eng A 2008;486:662–671.
[23] Narooei K, Karimi Taheri A. Strain field and extrusion load in ECAE process of bi-metal circular cross section. Applied Mathematical Modelling 2012;36:2128–41.
[24] Slamova M, Ocenasek V, Vander Voort G. Polarized light microscopy: utilization in the investigation of the recrystallization of aluminium alloys. Materials Characterization 2004;52:165–77.
[25] El-Danaf EA, Soliman MS, Almajid AA, El-Rayes MM. Enhancement of mechanical properties and grain size refinement of commercial purity aluminum 1050 processed by ECAP. Mater Sci Eng A 2007;458:226–34.